噻唑腙类IGF2BP2小分子抑制剂的设计、合成及生物活性研究

张诗迪[1,2], 马 赛[1,2], 王颖哲[1,2], 蔡媛倩[1,2], 张 艳[1,2], 尤启冬[1,2*], 郭小可[1,2*]

(1. 中国药科大学, 江苏省药物分子设计与成药性优化重点实验室, 江苏 南京 210009; 2. 中国药科大学药学院, 江苏 南京 210009)

摘要: 胰岛素样生长因子2 mRNA结合蛋白2 (insulin-like growth factor 2 mRNA binding protein 2, IGF2BP2) 是N^6-甲基腺苷 (N^6-methyladenosine, m^6A) 的识别蛋白, 介导了下游mRNA的稳定性, 是极具前景的抗肿瘤靶点。本研究基于课题组前期筛选的先导化合物**1g**, 以噻唑腙作为母核设计并合成了52个IGF2BP2小分子抑制剂, 其中**9g**、**10g**、**37g**、**47g**和**52g**等具有较好的靶标活性。该项工作是以噻唑腙为母核发展IGF2BP2小分子抑制剂的一次探索, 为后续相关研究奠定基础。

关键词: 噻唑腙衍生物; 胰岛素样生长因子2 mRNA结合蛋白2; N^6-甲基腺苷; 小分子抑制剂; 设计合成

中图分类号: R914 **文献标识码**: A **文章编号**: 0513-4870(2024)11-3006-11

Design, synthesis and biological activity study of thiazolehydrazone-based small molecule inhibitors of IGF2BP2

ZHANG Shi-di[1,2], MA Sai[1,2], WANG Ying-zhe[1,2], CAI Yuan-qian[1,2], ZHANG Yan[1,2], YOU Qi-dong[1,2*], GUO Xiao-ke[1,2*]

(*1. Jiangsu Key Laboratory of Drug Design and Optimization, China Pharmaceutical University, Nanjing 210009, China; 2. School of Pharmacy, China Pharmaceutical University, Nanjing 210009, China*)

Abstract: Insulin-like growth factor 2 mRNA binding protein 2 (IGF2BP2) is a recognition protein for N^6-methyladenosine (m^6A), mediating the stability of downstream mRNA, and is a promising anti-tumor target. Based on the lead compound **1g** from previous screening, this study designed and synthesized 52 IGF2BP2 small molecule inhibitors using thiazole hydrazone as the parent nucleus. Among them, **9g**, **10g**, **37g**, **47g** and **52g** showed good inhibitory activities. This work represents an initial exploration in the development of small molecule inhibitors targeting IGF2BP2, using thiazolehydrazone as the core structure. It lays a foundation for subsequent related research.

Key words: thiazole hydrazone derivative; insulin-like growth factor 2 mRNA binding protein 2; N^6-methyladenosine; small-molecule inhibitor; design and synthesis

表观遗传调控在细胞的生理过程中扮演着关键的作用[1], 而表观遗传失调已被证明与多种疾病尤其是癌症密切相关[2]。表观遗传学研究主要涉及到DNA、组蛋白和RNA的修饰[3]。目前已确认了100余种的RNA转录后修饰, 而N^6-甲基腺苷 (N^6-methyladenosine, m^6A) 被认为是真核生物信使RNA (message RNA, mRNA) 中最丰富的修饰[4,5]。随着m^6A甲基转移酶、去甲基酶和识别蛋白被逐步发现, 证明m^6A修饰具有可逆性[6]。其中m^6A阅读蛋白 (也被称为识别蛋白) 可通过调控RNA与蛋白之间的相互作用, 使m^6A修饰的RNA发挥特定的生物学功能[7]。这些阅读蛋白包括YTH结构域蛋白[8]、核不均一核糖蛋白 (heterogeneous nuclear

收稿日期: 2024-06-17; 修回日期: 2024-08-18.
基金项目: 国家自然科学基金资助项目 (82173673, 82473789).
*通讯作者 E-mail: youqd@cpu.edu.cn;
Tel: 13701475843, E-mail: kexin95@126.com
DOI: 10.16438/j.0513-4870.2024-0564

ribonucleoprotein, hnRNP)[9]、真核起始因子 (eukaryotic translation initiation factor, eIF)[10]和胰岛素样生长因子2 mRNA结合蛋白 (insulin-like growth factor-2 mRNA-binding proteins, IGF2BPs) 等家族[11,12]。IGF2BPs是一类RNA结合蛋白, 其家族成员包括IGF2BP1、IGF2BP2和IGF2BP3, 它们主要通过结合、调控特定mRNA的稳定性和翻译过程来参与包括细胞增殖、存活、代谢以及肿瘤的发生与发展等在内的多种生物进程[13] (图1A)。

IGF2BP2作为IGF2BPs蛋白家族成员——一种新的m^{6}A阅读蛋白, 可促进m^{6}A修饰的mRNA的稳定及翻译[13]。近年来多种研究证明, IGF2BP2可能诱导癌症的发生发展[4]。靶向IGF2BP2具有潜在的治疗急性髓系白血病[14]、肺腺癌[15]、结直肠癌[16]、胰腺癌[17]及肝细胞癌[18]的作用。随着对IGF2BP2蛋白结构及生理功能研究的深入, IGF2BP2已成为潜在的抗肿瘤药物靶标[19]。目前暂无高活性、高选择性的靶向IGF2BP2小分子抑制剂的报道, 因此, 进一步开展关于靶向IGF2BP2小分子抑制剂的研究具有重要意义。

为寻找全新结构的IGF2BP2小分子抑制剂, 基于竞争性荧光偏振实验 (fluorescence polarization assay, FP) 筛选商业化合物库和组内化合物库, 获得噻唑脲类化合物4EGI-1 (**1g**, 图1B)[20], 其对IGF2BP2与底物探针的结合显示出中等抑制活性 (IC_{50} = 23.06 ± 5.08 μmol·L^{-1}, 图1C)。为了进一步提高活性并探索构效关系, 本研究以**1g**为先导化合物, 分别针对其A环 (I系列) 和B环 (II系列) 引入不同取代基 (图1B), 共获得目标化合物52个, 通过核磁共振氢谱 (hydrogen nuclear magnetic resonance spectroscopy, ^{1}H NMR)、高分辨质谱 (high resolution mass spectroscopy, HRMS) 确证其化学结构, 并通过高效液相色谱 (high performance liquid chromatography, HPLC) 检测纯度。

结果与讨论

1 化学合成

化合物**1g**～**52g**的合成如合成路线1所示。以商业购买的取代芳醛**1a**～**28a**为原料, 在乙酸钠的存在下, 与*N*-乙酰甘氨酸在醋酐中经Erlenmeyer-Plöchl反应[21,22]得到中间体**1b**～**28b**, 随后在浓盐酸条件下开环得到关键中间体**1c**～**28c** (合成路线1A)。同时, 以商业购买的取代芳酮**1d**～**23d**为原料, 醋酸作溶剂, 经液溴溴化得到中间体**1e**～**23e**, 然后与硫代氨基脲经Hantzsch反应[23]得到关键中间体**1f**～**23f** (合成路线1B)。另将中间体**13f**经还原反应得到中间体**24f** (合成路线1C)。最后, 中间体**1c**～**28c**与中间体**1f**～**24f**或商业购买的**25f**在酸催化下进行缩合, 得到目标化合物**1g**～**52g** (合成路线1D、E), 理化常数及波谱数据见表1。

2 生物活性测试

使用实验室表达并纯化的IGF2BP2蛋白对52个目标化合物进行了基于FP的活性测试。I系列化合物相关结果如表2所示, II系列化合物相关结果如表3所示。其中大部分化合物的半数抑制浓度 (half maximal inhibitory concentration, IC_{50}) 在微摩尔级别, 特别是**9g**的活性 (IC_{50} = 0.97 ± 0.08 μmol·L^{-1}) 相较于**1g** (IC_{50} = 23.06 ± 5.08 μmol·L^{-1}) 有较大的提高。

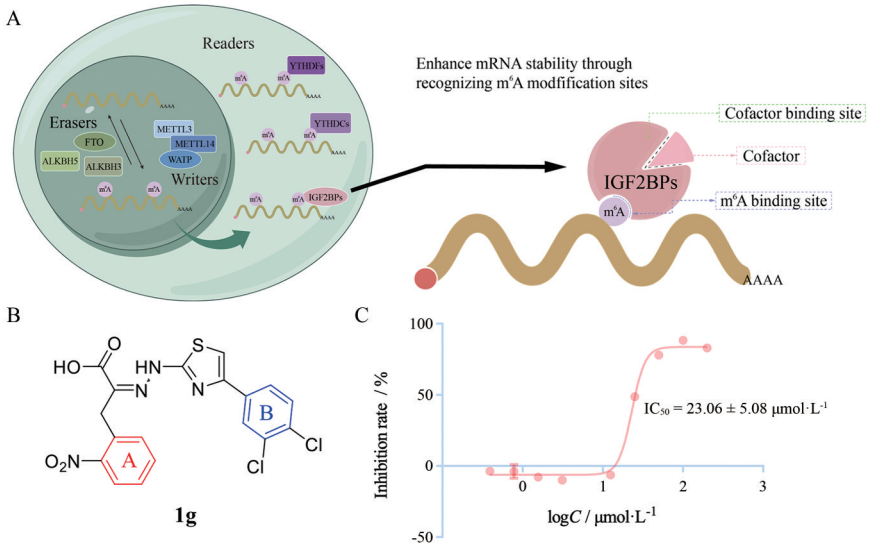

Figure 1 Discovery of the lead compound **1g**. A: Biological functions of IGF2BPs; B: Structure of compound **1g**; C: The inhibitory activity of **1g** against IGF2BP2 by fluorescence polarization assay. IGF2BPs: Insulin-like growth factor-2 mRNA-binding proteins

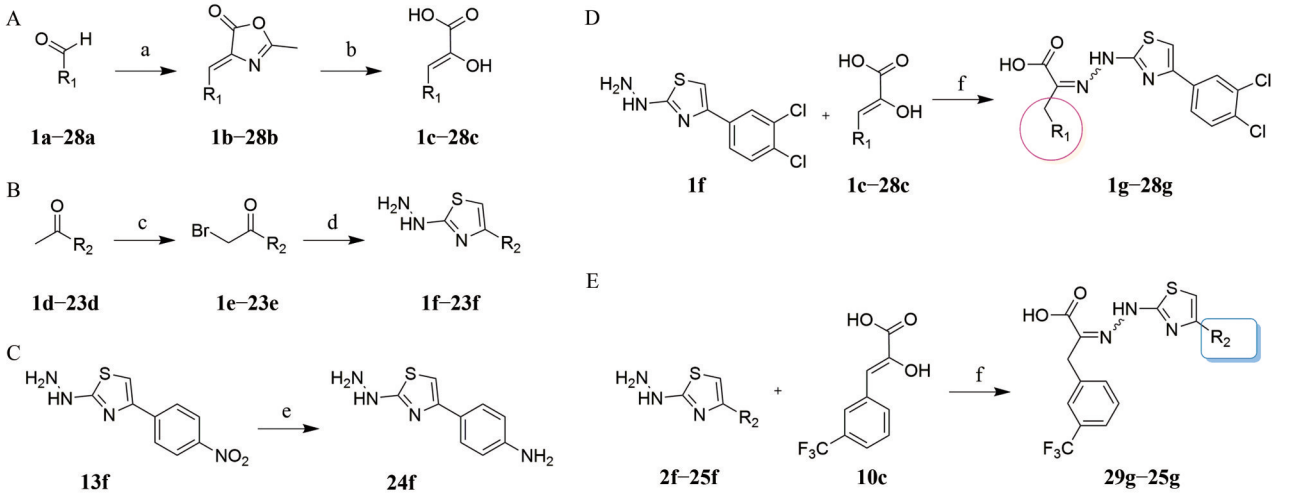

Scheme 1 The synthetic route of target compounds. Reagents and conditions: (a) *N*-acetyl glycine, sodium acetate, acetic anhydride, reflux, 4 h; (b) 34% HCl (aq.), reflux, 2 h; (c) Br_2, AcOH; (d) i. Thiosemicarbazide, 1,4-dioxane, rt, 4 h; ii. sat. Na_2CO_3 (aq.), rt, 30 min; (e) $SnCl_2·2H_2O$, EA, 80 ℃; (f) 5% AcOH/EtOH, reflux, 2 h

Table 1 m.p., ^{1}H NMR, ^{13}C NMR, HRMS (ESI) and HPLC elemental analysis data of target compounds

Cpd.	m.p., ^{1}H NMR, ^{13}C NMR, HRMS (ESI), HPLC
1g	m.p. 207.2−208.6 ℃. ^{1}H NMR (300 MHz, DMSO-d_6) δ_H: 13.25 (s, 1H), 12.12 (s, 1H), 8.06 (d, J = 2.2 Hz, 2H), 7.85−7.78 (m, 1H), 7.73−7.62 (m, 3H), 7.55 (d, J = 6.5 Hz, 2H), 4.33 (s, 1H), 4.20 (s, 1H). HRMS (ESI): calcd. for $C_{18}H_{12}C_{l2}N_4O_4S$ $[M-H]^-$ 448.988 3, found 448.987 1. Purity: 95.232% by HPLC (ACN/0.1% TFA = 50%, t_R = 8.291 min)
2g	m.p. 208.4−209.6 ℃. ^{1}H NMR (300 MHz, DMSO-d_6) δ_H: 13.13 (s, 1H), 12.15 (s, 1H), 8.12 (t, J = 2.1 Hz, 1H), 7.87 (dt, J = 8.5, 2.1 Hz, 1H), 7.69 (q, J = 4.8 Hz, 2H), 7.39−7.19 (m, 5H), 4.08 (s, 1H), 3.78 (s, 1H). HRMS (ESI): calcd. for $C_{18}H_{13}Cl_2N_3O_2S$ $[M-H]^-$ 404.003 2, found 404.002 2. Purity: 96.196% by HPLC (ACN/0.1% TFA = 50%, t_R = 8.716 min)
3g	m.p. 211.2−212.3 ℃. ^{1}H NMR (300 MHz, DMSO-d_6) δ_H: 13.21 (s, 1H), 12.15 (s, 1H), 8.10 (dd, J = 5.7, 2.0 Hz, 1H), 7.85 (dt, J = 8.4, 2.1 Hz, 1H), 7.77−7.55 (m, 2H), 7.45−6.98 (m, 4H), 4.06 (s, 1H), 3.83 (s, 1H). HRMS (ESI): calcd. for $C_{18}H_{12}Cl_2FN_3O_2S$ $[M-H]^-$ 421.993 8, found 421.992 9. Purity: 96.067% by HPLC (ACN/0.1% TFA = 50%, t_R = 8.168 min)
4g	m.p. 211.4−212.7 ℃. ^{1}H NMR (300 MHz, DMSO-d_6) δ_H: 12.73 (s, 1H), 12.17 (s, 1H), 8.08 (d, J = 2.1 Hz, 1H), 7.83 (dd, J = 8.5, 2.0 Hz, 1H), 7.67 (d, J = 8.6 Hz, 2H), 7.50 (dd, J = 5.8, 3.5 Hz, 1H), 7.28 (dd, J = 5.9, 3.5 Hz, 2H), 6.91 (dd, J = 5.8, 3.6 Hz, 1H), 4.08 (s, 2H). HRMS (ESI): calcd. for $C_{18}H_{12}Cl_3N_3O_2S$ $[M+H]^+$ 439.978 9, found 439.977 5. Purity: 95.934% by HPLC (ACN/0.1% TFA = 50%, t_R = 7.936 min)
5g	m.p. 202.2−203.4 ℃. ^{1}H NMR (300 MHz, DMSO-d_6) δ_H: 12.78 (s, 1H), 8.07 (d, J = 2.1 Hz, 1H), 7.82 (dd, J = 8.4, 2.1 Hz, 1H), 7.70−7.58 (m, 3H), 7.35 (dd, J = 6.6, 1.6 Hz, 2H), 7.22 (ddd, J = 7.9, 6.3, 2.8 Hz, 1H), 3.92 (s, 2H). HRMS (ESI): calcd. for $C_{18}H_{12}BrCl_2N_3O_2S$ $[M+H]^+$ 483.928 3, found 485.925 7. Purity: 96.165% by HPLC (ACN/0.1% TFA = 50%, t_R = 8.566 min)
6g	m.p. 205.1−206.3 ℃. ^{1}H NMR (300 MHz, DMSO-d_6) δ_H: 12.72 (s, 1H), 11.98 (s, 1H), 8.08 (d, J = 2.0 Hz, 1H), 7.82 (dd, J = 8.4, 2.1 Hz, 1H), 7.66 (d, J = 8.2 Hz, 2H), 7.26−7.19 (m, 1H), 7.12 (tt, J = 8.0, 6.4 Hz, 2H), 6.78−6.70 (m, 1H), 3.94 (s, 2H), 2.32 (s, 3H). HRMS (ESI): calcd. for $C_{19}H_{15}Cl_2N_3O_2S$ $[M+H]^+$ 420.033 5, found 420.033 4. Purity: 96.421% by HPLC (ACN/0.1% TFA = 50%, t_R = 8.537 min)
7g	m.p. 212.1−213.2 ℃. ^{1}H NMR (300 MHz, DMSO-d_6) δ_H: 13.20 (s, 1H), 12.23 (s, 1H), 8.10 (dd, J = 5.1, 2.0 Hz, 1H), 7.85 (dd, J = 8.4, 2.1 Hz, 1H), 7.68 (dd, J = 5.4, 3.5 Hz, 2H), 7.43−7.29 (m, 1H), 7.11−7.01 (m, 3H), 4.08 (s, 1H), 3.79 (s, 1H). HRMS (ESI): calcd. for $C_{18}H_{12}Cl_2FN_3O_2S$ $[M-H]^-$ 421.993 9, found 421.992 3. Purity: 95.916% by HPLC (ACN/0.1% TFA = 50%, t_R = 8.146 min)
8g	m.p. 203.4−204.6 ℃. ^{1}H NMR (300 MHz, DMSO-d_6) δ_H: 12.73 (s, 1H), 12.11 (s, 1H), 8.11 (t, J = 2.3 Hz, 1H), 7.86 (dt, J = 8.5, 2.0 Hz, 1H), 7.73−7.62 (m, 2H), 7.19 (t, J = 7.9 Hz, 1H), 7.03 (d, J = 7.7 Hz, 3H), 4.02 (s, 1H), 3.72 (s, 1H), 2.27 (s, 3H). HRMS (ESI): calcd. for $C_{19}H_{15}Cl_2N_3O_2S$ $[M-H]^-$ 418.018 9, found 418.017 9. Purity: 96.235% by HPLC (ACN/0.1%TFA = 50%, t_R = 8.579 min)
9g	m.p. 213.2−214.6 ℃. ^{1}H NMR (300 MHz, DMSO-d_6) δ_H: 12.94 (s, 1H), 12.22 (s, 1H), 8.11 (dd, J = 4.3, 2.0 Hz, 1H), 7.90−7.76 (m, 3H), 7.68 (d, J = 8.5 Hz, 2H), 7.53−7.40 (m, 2H), 4.12 (s, 1H), 3.83 (s, 1H). ^{13}C NMR (75 MHz, DMSO-d_6) δ_C: 169.30, 167.75, 165.99, 164.93, 140.05, 137.23, 135.40, 133.99, 133.45, 132.02, 131.45, 130.41, 129.59, 129.34, 127.94, 127.76, 126.09, 108.62, 31.36. HRMS (ESI): calcd. for $C_{19}H_{13}Cl_2N_3O_4S$ $[M-H]^-$ 447.993 1, found 447.992 5. Purity: 97.124% by HPLC (ACN/0.1%TFA = 50%, t_R = 7.825 min)
10g	m.p. 211.1−212.3 ℃. ^{1}H NMR (300 MHz, DMSO-d_6) δ_H: 12.87 (s, 1H), 12.25 (s, 1H), 8.10 (dd, J = 7.3, 2.1 Hz, 1H), 7.85 (dt, J = 8.7, 2.3 Hz, 1H), 7.60 (ddt, J = 24.7, 16.6, 8.6 Hz, 6H), 4.15 (s, 1H), 3.88 (s, 1H). HRMS (ESI): calcd. for $C_{19}H_{12}Cl_2F_3N_3O_2S$ $[M-H]^-$ 471.990 7, found 471.989 5. Purity: 96.267% by HPLC (ACN/0.1%TFA = 50%, t_R = 8.312 min)
11g	m.p. 205.2−206.4 ℃. ^{1}H NMR (300 MHz, DMSO-d_6) δ_H: 13.25 (s, 1H), 12.41 (s, 1H), 8.21−8.07 (m, 3H), 7.86 (ddd, J = 8.6, 3.9, 2.0 Hz, 1H), 7.77−7.60 (m, 4H), 4.21 (s, 1H), 3.95 (s, 1H). HRMS (ESI): calcd. for $C_{18}H_{12}Cl_2N_4O_4S$ $[M-H]^-$ 448.988 3, found 448.986 9. Purity: 95.146% by HPLC (ACN/0.1%TFA = 50%, t_R = 8.876 min)
12g	m.p. 207.1−208.2 ℃. ^{1}H NMR (300 MHz, DMSO-d_6) δ_H: 13.21 (s, 1H), 12.27 (s, 1H), 8.11 (dd, J = 5.4, 2.0 Hz, 1H), 7.89−7.79 (m, 3H), 7.74−7.53 (m, 4H), 4.18 (s, 1H), 3.92 (s, 1H), 3.22 (s, 3H). HRMS (ESI): calcd. for $C_{19}H_{15}Cl_2N_3O_4S_2$ $[M+Na]^+$ 505.977 3, found 505.978 5. Purity: 96.952% by HPLC (ACN/0.1%TFA = 50%, t_R = 8.268 min)

Continued

Cpd.	m.p., ^{1}H NMR, ^{13}C NMR, HRMS (ESI), HPLC
13g	m.p. 206.3−207.7 ℃. ^{1}H NMR (300 MHz, DMSO-d_6) δ_H: 13.17 (s, 1H), 12.15 (s, 1H), 8.12 (dd, J = 5.2, 2.0 Hz, 1H), 7.87 (dd, J = 8.4, 2.1 Hz, 1H), 7.74−7.63 (m, 2H), 7.33−7.22 (m, 2H), 7.22−7.10 (m, 2H), 4.05 (s, 1H), 3.77 (s, 1H). HRMS (ESI): calcd. for $C_{18}H_{12}Cl_2FN_3O_2S$ $[M-H]^-$ 421.993 9, found 421.992 5. Purity: 95.194% by HPLC (ACN/0.1%TFA = 50%, t_R = 8.346 min)
14g	m.p. 205.1−206.4 ℃. ^{1}H NMR (300 MHz, DMSO-d_6) δ_H: 13.13 (s, 1H), 12.09 (s, 1H), 8.10 (t, J = 1.9 Hz, 1H), 7.85 (dt, J = 8.5, 2.3 Hz, 1H), 7.67 (q, J = 4.6 Hz, 2H), 7.19 (t, J = 7.6 Hz, 1H), 7.07−6.95 (m, 3H), 4.02 (s, 1H), 3.72 (s, 1H), 2.27 (d, J = 2.7 Hz, 3H). HRMS (ESI): calcd. for $C_{19}H_{15}Cl_2N_3O_2S$ $[M-H]^-$ 418.018 9, found 418.017 7. Purity: 95.268% by HPLC (ACN/0.1%TFA = 50%, t_R = 8.826 min)
15g	m.p. 204.2−205.8 ℃. ^{1}H NMR (300 MHz, DMSO-d_6) δ_H: 12.85 (s, 1H), 12.18 (s, 1H), 8.10 (dd, J = 5.3, 2.0 Hz, 1H), 7.94−7.77 (m, 3H), 7.72−7.59 (m, 2H), 7.34 (dd, J = 14.7, 8.0 Hz, 2H), 4.13 (s, 1H), 3.82 (s, 1H). HRMS (ESI): calcd. for $C_{19}H_{13}Cl_2N_3O_4S$ $[M-H]^-$ 447.993 1, found 447.992 5. Purity: 95.051% by HPLC (ACN/0.1%TFA = 50%, t_R = 7.118 min)
16g	m.p. 207.4−208.7 ℃. ^{1}H NMR (300 MHz, DMSO-d_6) δ_H: 13.13 (s, 1H), 12.07 (s, 1H), 8.11 (dd, J = 3.6, 2.0 Hz, 1H), 7.86 (dt, J = 8.4, 1.5 Hz, 1H), 7.73−7.62 (m, 2H), 7.15 (dd, J = 8.7, 1.8 Hz, 2H), 6.87 (dd, J = 8.7, 1.3 Hz, 2H), 3.98 (s, 1H), 3.70 (t, J = 4.7 Hz, 4H). HRMS (ESI): calcd. for $C_{19}H_{15}Cl_2N_3O_3S$ $[M-H]^-$ 434.013 8, found 434.012 3. Purity: 96.271% by HPLC (ACN/0.1%TFA = 50%, t_R = 8.261 min)
17g	m.p. 206.0−207.2 ℃. ^{1}H NMR (300 MHz, DMSO-d_6) δ_H: 12.74 (s, 1H), 12.06 (s, 1H), 9.29 (d, J = 11.5 Hz, 1H), 8.12 (dd, J = 4.6, 2.0 Hz, 1H), 7.87 (dd, J = 8.4, 2.1 Hz, 1H), 7.74−7.63 (m, 2H), 7.04 (dd, J = 8.6, 2.9 Hz, 2H), 6.70 (d, J = 8.0 Hz, 2H), 3.94 (s, 1H), 3.64 (s, 1H). HRMS (ESI): calcd. for $C_{18}H_{13}Cl_2N_3O_3S$ $[M-H]^-$ 419.998 2, found 419.997 2. Purity: 97.629% by HPLC (ACN/0.1%TFA = 50%, t_R = 7.561 min)
18g	m.p. 206.5−207.9 ℃. ^{1}H NMR (300 MHz, DMSO-d_6) δ_H: 12.97 (s, 1H), 8.11 (t, J = 2.2 Hz, 1H), 7.86 (dt, J = 8.4, 1.9 Hz, 1H), 7.68 (dd, J = 7.6, 4.4 Hz, 2H), 6.99 (dd, J = 10.2, 8.0 Hz, 2H), 6.68 (dd, J = 13.7, 8.0 Hz, 2H), 3.90 (s, 1H), 3.63 (s, 1H). HRMS (ESI): calcd. for $C_{18}H_{14}Cl_2N_4O_2S$ $[M-H]^-$ 419.014 2, found 419.013 4. Purity: 95.081% by HPLC (ACN/0.1%TFA = 50%, t_R = 7.146 min)
19g	m.p. 204.3−205.6 ℃. ^{1}H NMR (300 MHz, DMSO-d_6) δ_H: 12.95 (s, 1H), 12.30 (s, 1H), 8.22 (dq, J = 8.8, 2.4 Hz, 2H), 8.11 (dd, J = 7.1, 2.0 Hz, 1H), 7.86 (dd, J = 8.4, 2.0 Hz, 1H), 7.74−7.60 (m, 2H), 7.52 (dd, J = 16.1, 8.7 Hz, 2H), 4.22 (s, 1H), 3.92 (s, 1H). HRMS (ESI): calcd. for $C_{18}H_{12}Cl_2N_4O_4S$ $[M-H]^-$ 448.988 4, found 448.986 6. Purity: 95.967% by HPLC (ACN/0.1%TFA = 50%, t_R = 8.591 min)
20g	m.p. 207.9−209.2 ℃. ^{1}H NMR (300 MHz, DMSO-d_6) δ_H: 13.12 (s, 1H), 12.26 (s, 1H), 8.12 (t, J = 2.4 Hz, 1H), 7.87 (dt, J = 8.5, 1.8 Hz, 1H), 7.70 (dt, J = 8.3, 4.8 Hz, 4H), 7.47 (dd, J = 14.6, 7.9 Hz, 2H), 4.17 (s, 1H), 3.89 (s, 1H). HRMS (ESI): calcd. for $C_{19}H_{12}Cl_2F_3N_3O_2S$ $[M-H]^-$ 471.990 7, found 471.988 7. Purity: 95.181% by HPLC (ACN/0.1%TFA = 50%, t_R = 8.173 min)
21g	m.p. 206.1−207.2 ℃. ^{1}H NMR (300 MHz, DMSO-d_6) δ_H: 13.20 (s, 1H), 8.60− 8.45 (m, 2H), 8.11 (dd, J = 8.1, 2.0 Hz, 1H), 7.90−7.78 (m, 2H), 7.73−7.62 (m, 2H), 7.45 (ddd, J = 24.7, 8.0, 5.0 Hz, 1H), 4.10 (s, 1H), 3.86 (s, 1H). HRMS (ESI): calcd. for $C_{17}H_{12}Cl_2N_4O_2S$ $[M-H]^-$ 404.998 5, found 404.998 2. Purity: 95.845% by HPLC (ACN/0.1%TFA = 50%, t_R = 8.491 min)
22g	m.p. 208.3−209.5 ℃. ^{1}H NMR (300 MHz, DMSO-d_6) δ_H: 13.86 (s, 1H), 12.44 (s, 1H), 8.61 (d, J = 5.0 Hz, 2H), 8.20 (dd, J = 4.7, 2.0 Hz, 1H), 7.95 (dd, J = 8.4, 2.1 Hz, 1H), 7.83−7.70 (m, 2H), 7.41 (dd, J = 44.8, 5.0 Hz, 2H), 4.20 (s, 1H), 3.92 (s, 1H). HRMS (ESI): calcd. for $C_{17}H_{12}Cl_2N_4O_2S$ $[M-H]^-$ 404.998 5, found 404.997 1. Purity: 95.324% by HPLC (ACN/0.1%TFA = 50%, t_R = 8.249 min)
23g	m.p. 204.1−205.2 ℃. ^{1}H NMR (300 MHz, DMSO-d_6) δ_H: 12.72 (s, 1H), 12.11 (s, 1H), 8.00 (dd, J = 5.6, 2.0 Hz, 1H), 7.75 (dt, J = 8.4, 2.3 Hz, 1H), 7.64−7.53 (m, 2H), 7.32−7.16 (m, 1H), 7.14−6.65 (m, 2H), 4.00 (s, 1H), 3.80 (s, 1H). HRMS (ESI): calcd. for $C_{18}H_{11}Cl_2F_2N_3O_2S$ $[M+H]^+$ 441.999 0, found 441.999 2. Purity: 95.948% by HPLC (ACN/0.1%TFA = 50%, t_R = 8.149 min)
24g	m.p. 208.2−209.3 ℃. ^{1}H NMR (300 MHz, DMSO-d_6) δ_H: 13.86 (s, 1H), 12.44 (s, 1H), 8.61 (d, J = 5.0 Hz, 2H), 8.20 (dd, J = 4.7, 2.0 Hz, 1H), 7.95 (dd, J = 8.4, 2.1 Hz, 1H), 7.83−7.70 (m, 2H), 7.41 (dd, J = 44.8, 5.0 Hz, 2H), 4.20 (s, 1H), 3.92 (s, 1H). HRMS (ESI): calcd. for $C_{19}H_{11}Cl_2F_4N_3O_2S$ $[M+H]^+$ 491.996 4, found 491.9960. Purity: 95.945% by HPLC (ACN/0.1%TFA = 50%, t_R = 8.159 min)
25g	m.p. 209.2−210.5 ℃. ^{1}H NMR (300 MHz, DMSO-d_6) δ_H: 12.99 (s, 1H), 8.10 (dd, J = 7.4, 2.1 Hz, 1H), 7.88−7.62 (m, 4H), 7.60−7.50 (m, 1H), 7.25 (dt, J = 9.0, 7.6 Hz, 1H), 4.08 (s, 1H), 3.88 (s, 1H). HRMS (ESI): calcd. for $C_{19}H_{12}Cl_2FN_3O_4S$ $[M+H]^+$ 467.998 9, found 467.998 0. Purity: 95.461% by HPLC (ACN/0.1%TFA = 50%, t_R = 7.591 min)
26g	m.p. 210.4−211.6 ℃. ^{1}H NMR (300 MHz, DMSO-d_6) δ_H: 13.54 (s, 1H), 12.29 (s, 1H), 8.16−8.02 (m, 1H), 7.83 (td, J = 8.0, 7.3, 2.0 Hz, 1H), 7.78−7.59 (m, 3H), 7.58−7.37 (m, 2H), 4.12 (s, 1H), 3.91 (s, 1H). HRMS (ESI): calcd. for $C_{19}H_{11}Cl_2F_4N_3O_2S$ $[M+H]^+$ 491.995 8, found 491.996 4. Purity: 95.895% by HPLC (ACN/0.1%TFA = 50%, t_R = 8.923 min)
27g	m.p. 212.1−213.2 ℃. ^{1}H NMR (300 MHz, DMSO-d_6) δ_H: 13.04 (s, 1H), 12.86 (s, 1H), 8.08 (s, 1H), 7.96−7.79 (m, 3H), 7.70−7.62 (m, 2H), 7.32 (t, J = 9.1 Hz, 1H), 4.08 (s, 1H), 3.89 (s, 1H). HRMS (ESI): calcd. for $C_{19}H_{12}Cl_2FN_3O_4S$ $[M+H]^+$ 467.998 2, found 468.000 1. Purity: 95.146% by HPLC (ACN/0.1%TFA = 50%, t_R = 7.150 min)
28g	m.p. 209.3−210.5 ℃. ^{1}H NMR (300 MHz, DMSO-d_6) δ_H: 13.07 (s, 1H), 12.32 (s, 1H), 8.08 (dd, J = 13.7, 2.0 Hz, 1H), 8.00 (d, J = 5.3 Hz, 2H), 7.94 (s, 1H), 7.83 (td, J = 8.7, 2.0 Hz, 1H), 7.73−7.59 (m, 2H), 4.23 (s, 1H), 4.04 (s, 1H). HRMS (ESI): calcd. for $C_{20}H_{11}Cl_2F_6N_3O_2S$ $[M+H]^+$ 541.993 2, found 541.992 6. Purity: 95.591% by HPLC (ACN/0.1%TFA = 50%, t_R = 8.257 min)
29g	m.p. 208.0−209.2 ℃. ^{1}H NMR (300 MHz, DMSO-d_6) δ_H: 13.28 (s, 1H), 12.21 (s, 1H), 7.85 (dd, J = 7.7, 3.4 Hz, 2H), 7.65−7.49 (m, 4H), 7.47−7.28 (m, 4H), 4.15 (s, 1H), 3.88 (s, 1H). HRMS (ESI): calcd. for $C_{19}H_{14}F_3N_3O_2S$ $[M+H]^+$ 406.083 8, found 406.082 8. Purity: 96.219% by HPLC (ACN/0.1%TFA = 50%, t_R = 8.824 min)
30g	m.p. 208.2−209.3 ℃. ^{1}H NMR (300 MHz, DMSO-d_6) δ_H: 13.20 (s, 1H), 12.26 (s, 1H), 7.99 (d, J = 8.7 Hz, 1H), 7.65−7.49 (m, 4H), 7.43−7.19 (m, 4H), 4.16 (s, 1H), 3.89 (s, 1H). HRMS (ESI): calcd. for $C_{19}H_{13}F_4N_3O_2S$ $[M+H]^+$ 424.074 4, found 424.075 0. Purity: 95.193% by HPLC (ACN/0.1%TFA = 50%, t_R = 8.781 min)
31g	m.p. 206.3−207.5 ℃. ^{1}H NMR (300 MHz, DMSO-d_6) δ_H: 12.72 (s, 1H), 12.24 (s, 1H), 7.84 (d, J = 7.3 Hz, 1H), 7.64−7.48 (m, 5H), 7.46−7.31 (m, 3H), 4.14 (s, 1H), 3.88 (s, 1H). HRMS (ESI): calcd. for $C_{19}H_{13}ClF_3N_3O_2S$ $[M+H]^+$ 440.044 8, found 440.044 0. Purity: 95.691% by HPLC (ACN/0.1%TFA = 50%, t_R = 8.245 min)
32g	m.p. 203.3−204.4 ℃. ^{1}H NMR (300 MHz, DMSO-d_6) δ_H: 13.14 (s, 1H), 8.58 (d, J = 4.8 Hz, 1H), 7.89 (dt, J = 14.8, 7.9 Hz, 2H), 7.69−7.48 (m, 5H), 7.34 (t, J = 5.9 Hz, 1H), 4.16 (s, 1H), 3.91 (s, 1H). HRMS (ESI): calcd. for $C_{18}H_{13}F_3N_4O_2S$ $[M+H]^+$ 407.079 0, found 407.078 1. Purity: 95.015% by HPLC (ACN/0.1%TFA = 50%, t_R = 8.228 min)

Continued

Cpd.	m.p., ^{1}H NMR, ^{13}C NMR, HRMS (ESI), HPLC
33g	m.p. 204.1−205.3 ℃. ^{1}H NMR (300 MHz, DMSO-d_6) δ_H: 13.03 (s, 1H), 12.38 (s, 1H), 10.84 (s, 1H), 7.84 (td, J = 7.8, 1.7 Hz, 1H), 7.67−7.46 (m, 5H), 7.21−7.10 (m, 1H), 6.95−6.80 (m, 2H), 4.15 (s, 1H), 3.90 (s, 1H). HRMS (ESI): calcd. for $C_{19}H_{14}F_3N_3O_3S$ $[M+H]^+$ 422.078 7, found 422.078 5. Purity: 95.117% by HPLC (ACN/0.1%TFA = 50%, t_R = 8.629 min)
34g	m.p. 202.1−203.3 ℃. ^{1}H NMR (300 MHz, DMSO-d_6) δ_H: 12.94 (s, 1H), 12.33 (s, 1H), 7.89 (s, 2H), 7.52 (d, J = 46.5 Hz, 5H), 7.24 (s, 2H), 4.15 (s, 1H), 3.89 (s, 1H). HRMS (ESI): calcd. for $C_{19}H_{13}F_4N_3O_2S$ $[M+H]^+$ 424.074 4, found 424.074 5. Purity: 96.018% by HPLC (ACN/0.1%TFA = 50%, t_R = 8.104 min)
35g	m.p. 206.3−207.5 ℃. ^{1}H NMR (300 MHz, DMSO-d_6) δ_H: 13.23 (s, 1H), 12.30 (s, 1H), 7.92−7.82 (m, 2H), 7.65−7.39 (m, 7H), 4.15 (s, 1H), 3.88 (s, 1H). HRMS (ESI): calcd. for $C_{19}H_{13}ClF_3N_3O_2S$ $[M+H]^+$ 440.044 8, found 440.043 8. Purity: 95.771% by HPLC (ACN/0.1%TFA = 50%, t_R = 8.263 min)
36g	m.p. 206.4−207.8 ℃. ^{1}H NMR (300 MHz, DMSO-d_6) δ_H: 13.91 (s, 1H), 9.24 (d, J = 4.9 Hz, 1H), 8.51 (s, 3H), 8.21 (dd, J = 12.8, 4.0 Hz, 5H), 4.77 (s, 1H), 4.50 (s, 1H). HRMS (ESI): calcd. for $C_{18}H_{13}F_3N_4O_2S$ $[M+H]^+$ 407.079 0, found 407.079 2. Purity: 95.142% by HPLC (ACN/0.1%TFA = 50%, t_R = 8.813 min)
37g	m.p. 207.2−208.4 ℃. ^{1}H NMR (300 MHz, DMSO-d_6) δ_H: 12.54 (s, 1H), 9.59 (s, 1H), 7.70−7.46 (m, 7H), 7.15 (s, 1H), 6.83−6.74 (m, 2H), 4.14 (s, 1H), 3.89 (s, 1H). HRMS (ESI): calcd. for $C_{19}H_{14}F_3N_3O_3S$ $[M+H]^+$ 422.078 7, found 422.081 6. Purity: 95.177% by HPLC (ACN/0.1%TFA = 50%, t_R = 8.183 min)
38g	m.p. 205.1−206.2 ℃. ^{1}H NMR (300 MHz, DMSO-d_6) δ_H: 13.31 (s, 2H), 9.76 (s, 1H), 8.24−7.83 (m, 8H), 7.72−7.48 (m, 1H), 4.32 (s, 2H). HRMS (ESI): calcd. for $C_{20}H_{14}F_3N_3O_4S$ $[M+H]^+$ 450.073 6, found 450.072 5. Purity: 95.834% by HPLC (ACN/0.1%TFA = 50%, t_R = 7.102 min)
39g	m.p. 209.2−210.3 ℃. ^{1}H NMR (300 MHz, DMSO-d_6) δ_H: 13.38 (s, 1H), 9.74 (s, 1H), 8.23 (s, 1H), 8.01−7.95 (m, 1H), 7.92−7.84 (m, 2H), 7.59 (d, J = 4.8 Hz, 2H), 7.16−7.07 (m, 2H), 6.51 (s, 1H), 4.26 (s, 2H), 3.85 (s, 3H). HRMS (ESI): calcd. for $C_{20}H_{16}F_3N_3O_3S$ $[M+H]^+$ 436.094 3, found 436.0933 7. Purity: 97.361% by HPLC (ACN/0.1%TFA = 50%, t_R = 8.445 min)
40g	m.p. 206.1−207.2 ℃. ^{1}H NMR (300 MHz, DMSO-d_6) δ_H: 12.95 (s, 1H), 12.32 (s, 1H), 8.28 (t, J = 8.8 Hz, 2H), 8.12 (d, J = 8.5 Hz, 2H), 7.85 (d, J = 4.9 Hz, 1H), 7.57 (ddd, J = 20.1, 11.3, 4.7 Hz, 4H), 4.16 (s, 1H), 3.91 (s, 1H). HRMS (ESI): calcd. for $C_{19}H_{13}F_3N_4O_4S$ $[M+H]^+$ 451.068 9, found 451.068 1. Purity: 95.184% by HPLC (ACN/0.1%TFA = 50%, t_R = 8.739 min)
41g	m.p. 211.1−212.3 ℃. ^{1}H NMR (300 MHz, DMSO-d_6) δ_H: 13.07 (s, 1H), 12.25 (s, 1H), 8.08−8.00 (m, 2H), 7.87 (dd, J = 8.3, 5.2 Hz, 2H), 7.76 (d, J = 6.4 Hz, 1H), 7.65−7.46 (m, 4H), 4.16 (s, 1H), 3.90 (s, 1H). HRMS (ESI): calcd. for $C_{20}H_{13}F_3N_4O_2S$ $[M+H]^+$ 431.079 0, found 431.078 7. Purity: 96.226% by HPLC (ACN/0.1%TFA = 50%, t_R = 8.816 min)
42g	m.p. 207.1−208.2 ℃. ^{1}H NMR (300 MHz, DMSO-d_6) δ_H: 12.99 (s, 1H), 12.29 (s, 1H), 7.76−7.65 (m, 1H), 7.66−7.54 (m, 5H), 7.53−7.38 (m, 2H), 7.16 (dt, J = 9.9, 5.0 Hz, 1H), 4.15 (s, 1H), 3.89 (s, 1H). HRMS (ESI): calcd. for $C_{19}H_{13}F_4N_3O_2S$ $[M+H]^+$ 424.074 4, found 424.074 8. Purity: 95.988% by HPLC (ACN/0.1%TFA = 50%, t_R = 8.502 min)
43g	m.p. 207.2−208.3 ℃. ^{1}H NMR (300 MHz, DMSO-d_6) δ_H: 13.08 (s, 1H), 12.32 (s, 1H), 7.95−7.84 (m, 2H), 7.64−7.47 (m, 4H), 7.43 (d, J = 3.4 Hz, 1H), 7.31−7.17 (m, 2H), 4.15 (s, 1H), 3.89 (s, 1H). HRMS (ESI): calcd. for $C_{19}H_{13}ClF_3N_3O_2S$ $[M+H]^+$ 440.044 8, found 440.043 9. Purity: 96.117% by HPLC (ACN/0.1%TFA = 50%, t_R = 8.436 min)
44g	m.p. 211.2−212.4 ℃. ^{1}H NMR (300 MHz, DMSO-d_6) δ_H: 13.03 (s, 1H), 9.08 (s, 1H), 8.52 (s, 1H), 8.23 (d, J = 8.1 Hz, 1H), 7.68−7.46 (m, 6H), 4.16 (s, 1H), 3.90 (s, 1H). HRMS (ESI): calcd. for $C_{18}H_{13}F_3N_4O_2S$ $[M+H]^+$ 407.079 0, found 407.077 6. Purity: 95.901% by HPLC (ACN/0.1%TFA = 50%, t_R = 8.195 min)
45g	m.p. 208.0−209.2 ℃. ^{1}H NMR (300 MHz, DMSO-d_6) δ_H: 12.92 (s, 1H), 12.24 (s, 1H), 9.51 (s, 1H), 7.65−7.46 (m, 4H), 7.36 (s, 1H), 7.30−7.13 (m, 3H), 6.72 (d, J = 7.9 Hz, 1H), 4.15 (s, 1H), 3.90 (s, 1H). HRMS (ESI): calcd. for $C_{19}H_{14}F_3N_3O_3S$ $[M+H]^+$ 422.078 7, found 422.078 9. Purity: 95.292% by HPLC (ACN/0.1%TFA = 50%, t_R = 8.026 min)
46g	m.p. 205.2−206.3 ℃. ^{1}H NMR (300 MHz, DMSO-d_6) δ_H: 13.43 (s, 1H), 13.09 (s, 1H), 12.29 (s, 1H), 8.55−8.37 (m, 1H), 8.27−8.07 (m, 1H), 8.00−7.84 (m, 1H), 7.56 (dtd, J = 12.4, 9.0, 7.8, 3.9 Hz, 6H), 4.15 (s, 1H), 3.88 (s, 1H). HRMS (ESI): calcd. for $C_{20}H_{14}F_3N_3O_4S$ $[M+H]^+$ 450.073 6, found 450.073 2. Purity: 95.723% by HPLC (ACN/0.1%TFA = 50%, t_R = 7.273 min)
47g	m.p. 204.4−205.6 ℃. ^{1}H NMR (300 MHz, DMSO-d_6) δ_H: 12.92 (s, 1H), 12.21 (s, 1H), 10.04 (d, J = 3.7 Hz, 1H), 7.66−7.43 (m, 6H), 7.29 (d, J = 4.9 Hz, 1H), 6.96 (td, J = 8.8, 4.0 Hz, 1H), 4.14 (s, 1H), 3.88 (s, 1H). HRMS (ESI): calcd. for $C_{19}H_{13}F_4N_3O_3S$ $[M+H]^+$ 440.069 3, found 440.069 1. Purity: 95.519% by HPLC (ACN/0.1%TFA = 50%, t_R = 8.523 min)
48g	m.p. 203.1−204.2 ℃. ^{1}H NMR (300 MHz, DMSO-d_6) δ_H: 12.93 (s, 1H), 12.22 (s, 1H), 10.37 (s, 1H), 7.82 (dd, J = 8.2, 2.2 Hz, 1H), 7.68−7.46 (m, 5H), 7.32 (s, 1H), 6.99 (dd, J = 8.5, 2.9 Hz, 1H), 4.14 (s, 1H), 3.89 (s, 1H). HRMS (ESI): calcd. for $C_{19}H_{13}ClF_3N_3O_3S$ $[M+H]^+$ 456.039 7, found 456.039 0. Purity: 95.786% by HPLC (ACN/0.1%TFA = 50%, t_R = 8.076 min)
49g	m.p. 207.3−208.4 ℃. ^{1}H NMR (300 MHz, DMSO-d_6) δ_H: 13.20 (s, 1H), 12.25 (s, 1H), 10.11 (s, 1H), 7.79 (td, J = 9.1, 4.3 Hz, 1H), 7.64−7.43 (m, 4H), 7.10 (dd, J = 4.8, 2.4 Hz, 1H), 6.66 (dtt, J = 11.4, 4.1, 2.4 Hz, 2H), 4.15 (s, 1H), 3.88 (s, 1H). HRMS (ESI): calcd. for $C_{19}H_{13}F_4N_3O_3S$ $[M+H]^+$ 440.069 3, found 440.069 2. Purity: 95.912% by HPLC (ACN/0.1%TFA = 50%, t_R = 8.519 min)
50g	m.p. 207.1−208.2 ℃. ^{1}H NMR (300 MHz, DMSO-d_6) δ_H: 12.75 (s, 1H), 12.23 (s, 1H), 10.09 (s, 1H), 7.69−7.46 (m, 5H), 7.23 (s, 1H), 6.89 (t, J = 2.4 Hz, 1H), 6.80 (dd, J = 8.7, 2.5 Hz, 1H), 4.13 (s, 1H), 3.89 (s, 1H). HRMS (ESI): calcd. for $C_{19}H_{13}ClF_3N_3O_3S$ $[M+H]^+$ 456.039 7, found 456.039 0. Purity: 95.529% by HPLC (ACN/0.1%TFA = 50%, t_R = 8.157 min)
51g	m.p. 208.0−209.2 ℃. ^{1}H NMR (300 MHz, DMSO-d_6) δ_H: 13.42 (s, 1H), 11.98 (s, 1H), 7.55 (ddd, J = 20.7, 7.9, 4.3 Hz, 6H), 6.98 (s, 1H), 6.59 (d, J = 8.3 Hz, 2H), 4.14 (s, 1H), 3.88 (s, 1H). HRMS (ESI): calcd. for $C_{19}H_{15}F_3N_4O_2S$ $[M+H]^+$ 421.094 7, found 421.093 9. Purity: 95.017% by HPLC (ACN/0.1%TFA = 50%, t_R = 7.081 min)
52g	m.p. 205.4−206.7 ℃. ^{1}H NMR (300 MHz, DMSO-d_6) δ_H: 12.61 (s, 1H), 7.76 (dd, J = 20.5, 7.8 Hz, 1H), 7.65−7.49 (m, 4H), 7.48−7.26 (m, 2H), 7.24−7.08 (m, 1H), 4.14 (s, 1H), 3.92 (s, 1H). HRMS (ESI): calcd. for $C_{17}H_{12}F_3N_3O_2S$ $[M+H]^+$ 380.068 1, found 380.067 3. Purity: 95.196% by HPLC (ACN/0.1%TFA = 50%, t_R = 8.537 min)

Table 2 Structures and inhibitory activities of **1g**–**28g**. $n = 2, \bar{x} \pm s$

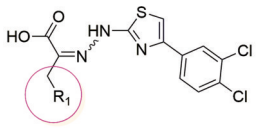

Cpd.	R_1	IC_{50}/μmol·L^{-1}	Cpd.	R_1	IC_{50}/μmol·L^{-1}
1g		23.06 ± 5.08	**2g**		11.35 ± 1.77
3g		7.53 ± 0.37	**4g**		10.48 ± 1.59
5g		45.40 ± 5.23	**6g**		17.03 ± 0.45
7g		10.48 ± 2.92	**8g**		8.01 ± 0.47
9g		0.97 ± 0.08	**10g**		6.81 ± 0.64
11g		7.17 ± 0.38	**12g**		10.48 ± 1.15
13g		11.35 ± 1.26	**14g**		13.62 ± 0.72
15g		3.24 ± 0.59	**16g**		17.03 ± 1.83
17g		17.03 ± 2.26	**18g**		27.24 ± 3.09
19g		8.01 ± 0.73	**20g**		11.35 ± 1.75
21g		13.26 ± 1.07	**22g**		9.73 ± 0.56
23g		12.38 ± 1.06	**24g**		6.75 ± 0.53
25g		1.70 ± 0.11	**26g**	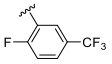	6.49 ± 0.31
27g	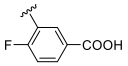	5.24 ± 0.45	**28g**	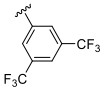	6.49 ± 0.89

3 化合物的构效关系研究

基于化合物**1g**的结构, 将其拆分为两个部分: A环与B环, 分别进行优化, 以期得到活性更优的IGF2BP2小分子抑制剂。设计并合成了两个系列的噻唑脲类化合物, 共获得了28个A环改造衍生物 (I系列) 和24个B环改造衍生物 (II系列)。

3.1 I系列化合物的构效关系研究 针对A环进行了一系列取代基的替换, 设计并合成化合物**1g**～**18g**。随后, 通过FP实验进行生物活性测试, 并对活性结果进行构效关系分析: ① 从整体来看, A环带有吸电子基的化合物较带有给电子基的化合物活性更好, 带酸性基团的化合物较带碱性基团的化合物活性更好。② 从各取代位置来看, A环邻位随着位阻的增大化合物的活性降低 (如**3g**～**6g**); 间位酸性基团的引入有利于化合

Table 3 Structures and inhibitory activities of **29g**−**52g**. $n = 2$, $\bar{x} \pm s$

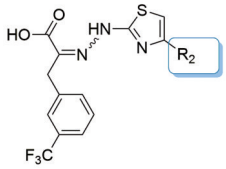

Cpd.	R_2	IC_{50}/μmol·L^{-1}	Cpd.	R_2	IC_{50}/μmol·L^{-1}
29g		9.88 ± 1.32	**30g**		7.12 ± 0.87
31g		5.82 ± 0.46	**32g**		26.35 ± 1.89
33g		15.21 ± 1.76	**34g**		7.08 ± 0.83
35g		10.19 ± 1.52	**36g**		>100
37g		1.90 ± 0.21	**38g**		9.55 ± 1.23
39g		>200	**40g**		6.77 ± 0.53
41g		14.55 ± 1.23	**42g**		7.07 ± 0.67
43g		8.77 ± 0.94	**44g**		28.93 ± 2.25
45g		9.61 ± 1.06	**46g**		4.81 ± 0.59
47g		1.33 ± 0.08	**48g**		4.36 ± 0.33
49g		5.81 ± 0.61	**50g**		9.45 ± 0.27
51g		4.48 ± 0.12	**52g**		1.41 ± 0.54

物活性的提高 (如 **9g**); 疏水基团会随着位阻的增大使化合物活性有所提高 (如 **7g**、**8g** 和 **9g**); 对位酸性基团的引入也能使得化合物活性有所提高, 而这种活性的提高没有间位取代明显 (如 **15g**)。这些发现为进一步的药物设计和优化提供了重要的指导。

在构效关系研究中, 发现硝基对小分子的抑制活性具有重要影响 (如 **1g**、**11g** 和 **19g**), 考虑到硝基基团潜在的毒性等不利影响, 采用生物电子等排策略进行了后续的结构优化。综合考虑取代基大小等因素后, 最终选择了吡啶基及邻二氟苯基对硝基苯进行替换, 设计合成了化合物 **21g**～**23g**, 并通过 FP 实验对它们的靶标活性进行测试, 结果如表 2 所示, 然而活性并没有明显改善。

基于上述构效关系分析的结果, 选择活性较好的两个化合物 **9g** 和 **10g** 进行分子对接研究, 预测它们与 IGF2BP2 蛋白可能的结合模式 (图 2A、B)。对接结果显示, **9g** 可能与蛋白空腔内的碱性氨基酸 Arg576 形成离子键相互作用从而使活性提高 (图 2A); **10g** 与空腔内的疏水氨基酸形成广泛的疏水作用可能使活性提高 (图 2B)。

然后, 尝试对 **9g** 和 **10g** 进行改造, 以期进一步提高活性。考虑到对接结果显示 **9g** 和 **10g** 能够分别通过离

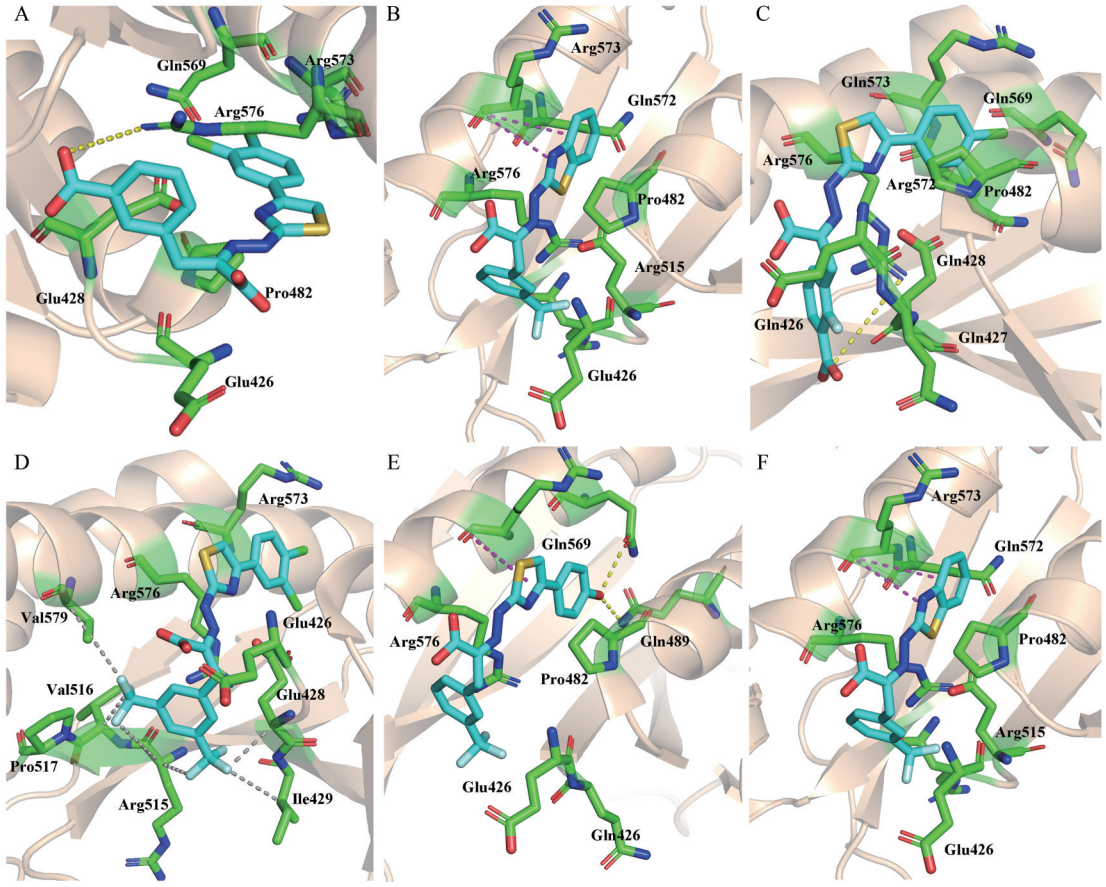

Figure 2 The predicted binding mode of different molecules with IGF2BP2 protein (PDB: 6ROL) by molecular docking. A: **9g**; B: **10g**; C: **25g**; D: **28g**; E: **37g**; F: **52g**. Yellow dash lines indicated ionic bonds, gray dash lines indicated hydrophobic interactions, magenta dash lines indicated pi-cation stacked interactions

子键和疏水作用与蛋白形成相互作用, 于是分别尝试增强这两种作用以提高活性: 针对离子键作用, 设想通过在酸性基团的邻位引入吸电子基团而使其酸性增强, 从而增强离子键的作用, 尝试在羧基邻位引入小位阻吸电子基团F原子, 以避免引入大位阻取代基而导致活性下降; 针对疏水作用, 考虑通过增加疏水基团的数量或者放大基团大小, 以增加分子与靶点蛋白的疏水相互作用。基于以上假设, 尝试引入三氟甲基, 以增强分子与靶标的相互作用 (图2C、D)。根据上述思路, 设计并合成了化合物**23g**～**28g**, 然而活性没有得到明显的改善。

3.2 II系列化合物的构效关系研究 本阶段, 选择保留A环的三氟甲基对B环进行一系列取代基的替换。首先, 设计并合成了化合物**29g**～**39g**和**42g**～**46g**, 通过FP实验对它们的靶标活性进行测试, 活性结果如表3所示, 并对构效关系进行分析: ① B环邻位引入小位阻疏水基团较亲水基团活性更好, 而吡啶基的引入导致化合物的活性大幅度下降 (如**29g**～**33g**); ② B环间位引入取代基会使得活性有微弱的提升, 其基团优先顺序为酸性基团 > 疏水基团 > 碱性基团, 吡啶基的引入导致活性大幅下降 (如**42g**～**46g**); ③ B环对位引入小位阻疏水基团对活性有微弱改善, 羟基的引入使得活性有明显提高 (如**34g**～**39g**)。

鉴于B环对位的羟基取代对活性的重要贡献, 通过分子对接对**37g**与IGF2BP2蛋白的可能得结合模式进行分析, 寻找结合腔内可能与小分子形成重要相互作用的氨基酸 (图2E), 以期提高化合物的活性。分子对接结果显示, **37g**中B环羟基的O原子可能与Gln489相互作用, O-H与Gln569相互作用; 另外还观察到, 噻唑环和苯环可能与一些氨基酸 (如Arg573等) 产生阳离子-π堆叠作用, 基于上述假设, 接下来考虑从增强这两个方面的作用来尝试进一步提高活性。

于是设计并合成了化合物**47g**～**50g**及**52g**, ① 对于氢键作用, 通过在羟基的邻位引入吸电子基, 以增加羟基的酸性, 从而增强其氢键供体的能力; 考虑到位阻效应, 选择在氢键邻位引入F原子, 设计合成化合物**47g**及一系列疏水基团对照; ② 对阳离子-π堆叠作用, 尝试通过在小分子芳香环上引入额外的环状结构以扩

大芳香环大小, 从而增强小分子与靶点之间的阳离子-π相互作用。将4-苯基噻唑环改为苯并噻唑环, 以**29g**作为对照设计合成了化合物**52g**。

FP实验结果显示, 在B环羟基的邻位或对位引入吸电子基, 活性提高 (如**47g**较**37g**活性提高), 初步证实上述假设; 另外**52g**较**29g**活性明显提高, 表明该区域的阳离子-π堆叠作用对活性有重要影响。上述实验结果, 进一步验证了**52g**与IGF2BP2蛋白的分子对接结果 (图2F)。最后, 尝试通过生物电子等排策略对**37g**中B环的羟基进行替换, 进一步对结构进行优化来改善小分子的亲和力。选择了羟基的生物电子等排体 (如氨基和氰基等), 设计合成化合物**37g**、**40g**、**41g**和**51g**, 并通过FP实验对它们的靶标活性进行测试。结果显示, 这些基团的引入并未能使活性改善。

4 结论

前期通过荧光偏振高通量筛选方法对组内的化合物库进行筛选, 获得了分子量较小且具有中等抑制活性的苗头化合物**1g** (IC_{50} = 23.06 ± 5.08 μmol·L^{-1})。在化合物**1g**的基础上, 通过分子对接对其结合模式进行分析, 并展开进一步的结构优化工作, 最终得到活性大幅提高的I系列化合物**9g** (IC_{50} = 0.97 ± 0.08 μmol·L^{-1})、**10g** (IC_{50} = 6.81 ± 0.64 μmol·L^{-1}) 和II系列化合物**47g** (IC_{50} = 1.33 ± 0.08 μmol·L^{-1}) 和**52g** (IC_{50} = 1.41 ± 0.54 μmol·L^{-1})。通过噻唑脲系列化合物的优化工作, 初步总结了构效关系, 为进一步开展噻唑脲类IGF2BP2小分子抑制剂研究提供了参考。

该项工作是以噻唑脲为母核发展IGF2BP2小分子抑制剂的一次探索, 相关活性化合物可以作为先导化合物进行进一步的结构优化, 以获得活性更高的IGF2BP2小分子抑制剂。

实验部分

本论文所涉及中间体及终产物的^{1}H NMR和^{13}C NMR核磁共振图谱由Bruker AV-300 (300 MHz)核磁共振仪测定, 测定溶剂为氘代二甲基亚砜 (DMSO-d_6) 或者氘代氯仿 ($CDCl_3$), 内标为四甲基硅烷 (TMS), 熔点由METTLER TOLEDO的MP50 Melting Point System熔点仪进行测定; 质谱由Advion小型台式质谱仪Expression CMS (EI-MS)、Agilent公司的1946A-MSD型质谱仪 (ESI-MS)、Water Q-Tof型质谱仪 (HRMS)测定; 纯度由岛津高效液相 (HPLC) 测定, 所用色谱柱为Agilent C18 (4.6 mm × 250 mm, 5 μm) 型反相柱; 柱层析所用的硅胶目数为200～300目 (青岛海洋化学工厂), 洗脱剂所用溶剂为石油醚、二氯甲烷、乙酸乙酯、甲醇; 薄层层析色谱 (TLC) 采用0.25 mm GF254薄层色谱硅胶板进行检测, 展开剂所用溶剂为石油醚、二氯甲烷、乙酸乙酯、甲醇, 通过ZF7型三用紫外分析仪观察; FP实验所用仪器为SpectaMax Multi-Mode Microplate Reader (Molecular Devices), 使用的激发光波长及发射光波长为485和535 nm。

FP实验所使用的蛋白为实验室表达并纯化的IGF2BP2蛋白, 使用的探针为5′-ATTGTCA (m^6A) CAGCAGA-FAM-3′, 实验所用的缓冲体系为硼酸−硼砂体系 (0.1 mmol·L^{-1}四硼酸钠, 1.6 mmol·L^{-1}硼酸, pH = 7.4), 实验所用的384孔黑板为Corning生产。化学实验中涉及的所有试剂原料均为化学纯或分析纯, 未注明具体来源的试剂和溶剂为市场购买的常规试剂 (毕得医药、乐研试剂、上海泰坦、安耐吉化学等公司), 储存条件按照原料或商品制造厂商所建议的条件。

1 化学合成

1.1 中间体1b～28b的合成 取原料**1a**～**28a** (6.62 mmol), *N*-乙酰甘氨酸 (3.87 g, 33.09 mmol), 乙酸钠 (2.71 g, 33.09 mmol) 加入圆底烧瓶中, 加入乙酸酐20 mL, 升温至130 ℃, 加热反应4 h。TLC监测, 原料**1a**～**28a**反应完全后, 将反应液倒入20 mL冰水中, 继续搅拌15 min, 有大量黑色油状物生成。用乙酸乙酯和水萃取, 有机相用无水硫酸钠干燥, 减压蒸馏除去溶剂, 柱层析纯化得到中间体**1b**～**28b** (产率84.42%～87.21%)。

1.2 中间体1c～28c的合成 取化合物**1b**～**28b** (4.31 mmol) 于圆底烧瓶中, 加入34%盐酸水溶液, 升温至100 ℃反应2 h, 溶液由浑浊变澄清透明, 趁热过滤掉残渣, 滤液放置室温冷却过夜, 第二天有白色晶体析出, 过滤, 滤饼在烘灯下烘干, 得到中间体**1c**～**28c**白色固体 (产率52.37%～60.61%)。

1.3 中间体1e～23e的合成 取原料**1d**～**23d** (5.29 mmol) 于圆底烧瓶中, 加入20 mL冰醋酸, 冰浴下搅拌10 min, 缓慢加入液溴 (271 μL, ρ = 3.12 g·cm^{-3}, 5.29 mmol), 待体系稳定后移至室温继续反应4 h。TLC监测原料**1d**～**23d**反应完全, 向反应液加入适量冰水, 继续搅拌15 min, 体系澄清, 用乙酸乙酯和水萃取, 有机相用无水硫酸钠干燥, 减压蒸馏除去溶剂, 柱层析纯化得到中间体**1e**～**23e** (产率90.98%～98.07%)。

1.4 中间体1f～23f的合成 取原料**1e**～**23e** (3.73 mmol), 硫代氨基脲 (340 mg, 3.73 mmol) 于圆底烧瓶中, 加入1,4-二氧六环溶液20 mL室温搅拌8 h, 有大量白色沉淀析出, TLC监测原料**1e**～**23e**反应完全, 过滤, 滤饼干燥后倒入圆底烧瓶中, 加入25 mL饱和碳酸钠水溶液搅拌15 min, 白色沉淀慢慢溶解, 继续搅拌

有黄色沉淀析出, 过滤, 干燥滤饼, 得到中间体**1f**～**23f** (产率84.03～90.95%)。

1.5 中间体24f的合成 取化合物**13f** (72 mg, 0.30 mmol), 二水氯化亚锡(343 mg, 1.52 mmol) 于圆底烧瓶中, 加入10 mL乙酸乙酯, 80 ℃加热搅拌6 h, TLC监测原料反应完全, 将反应液冷却至室温, 加入20 mL水, 冰浴下加入5 mol·L^{-1} NaOH水溶液调pH至10, 体系中有白色黏稠油状物析出, 保持冰浴搅拌10 min, 抽滤, 滤饼用乙酸乙酯洗2～3次, 收集滤液用乙酸乙酯和水萃取, 有机相用无水硫酸钠干燥后减压蒸馏, 得到棕色油状物。制砂, 经柱层析纯化得到中间体**24f** (19 mg, 产率30.22%)。

1.6 1g～28g的合成 取中间体**1c**～**28c** (1.43 mmol), 中间体**1f** (373 mg, 1.43 mmol) 于50 mL圆底烧瓶中, 加入5% AcOH/EtOH 15 mL, 升温至90 ℃反应2 h。冷却至室温, 有黄色沉淀析出, 过滤, 滤饼干燥后用乙醇重结晶, 得到化合物**1g**～**28g**的*E*/*Z*式异构体 (产率52.36%～58.86%)。

1.7 29g～52g的合成 以中间体**10c** (300.00 mg, 1.29 mmol) 和中间体**2f**～**24f**或购买的**25f** (1.29 mmol) 为反应原料, 按照1.6所述方法合成, 得到目标产物**29g**～**52g**的*E*/*Z*式异构体 (产率65.37%～70.82%)。

化合物理化常数和波谱数据见表1。

2 生物活性评价——IGF2BP2蛋白的FP评价方法

实验所用测试体系为60 μL, 其中蛋白、化合物、探针各20 μL, 化合物以3倍梯度稀释10～14个浓度, 每个浓度设置1个复孔。空白对照为20 μL探针 + 40 μL缓冲溶液, 阴性对照为20 μL蛋白 + 20 μL探针 + 20 μL缓冲溶液, 加完板后用锡箔纸将384孔板包住, 在摇床上室温振荡30 min, 使用仪器测定荧光偏振值, 并根据公式 (1) 计算抑制率。使用GraphPad Prism计算化合物的IC_{50}值。

$$抑制率\ (\%) = [1 - (P_{obs} - P_{min}) / (P_{max} - P_{min})] \times 100 \quad (1)$$

其中, P_{max}、P_{min}、P_{obs}分别为IGF2BP2和荧光探针孔的偏振值、荧光探针孔的偏振值及含有抑制剂孔的偏振值。

3 分子对接方法

应用从Protein Data Bank中下载IGF2BP2 (KH3和KH4结构域) 的蛋白质晶体结构 (PDB: 6ROL), 并借助Discovery Studio软件的Prepare Protein模块对蛋白结构进行初步处理, 接着通过Receptor-Ligand Interactions/Define and Edit Binding Site/From Receptor Cavities模块寻找可能的结合位点, 结合软件打分选取打分最高的潜在小分子结合位点, 并调节SBD_Site_Sphere的半径至10 Å。随后通过Prepare Ligand模块对小分子进行处理, 通过LibDock方法对小分子配体和蛋白进行分子对接, 然后对打分结果进行分析, 得到可能的小分子配体和蛋白的结合模式。

作者贡献: 张诗迪负责化合物的合成、数据的整理及文章撰写; 马赛负责化合物合成、分子对接和FP靶标活性测试工作; 王颖哲、蔡媛倩和张艳负责化合物的筛选、FP测试和可视化分析; 尤启冬负责课题规划、实验指导; 郭小可负责实验指导、文章修改及校对。

利益冲突: 本文所有作者声明不存在利益冲突关系。

References

[1] Zhang FP, Wang YY, Cheng XT, et al. Study on the molecular mechanism of anti-HBV effect of active fractions of wild chrysanthemum based on epigenetics and metabolomics [J]. Acta Pharm Sin (药学学报), 2022, 57: 2352-2363.

[2] Yang J, Xu J, Wang W, et al. Epigenetic regulation in the tumor microenvironment: molecular mechanisms and therapeutic targets [J]. Signal Transduct Target Ther, 2023, 8: 210.

[3] Chen XF, Xu HQ, Shu X, et al. Mapping epigenetic modifications by sequencing technologies [J]. Cell Death Differ, 2023. DOI: 10.1038/s41418-023-01213-1.

[4] Huang HL, Weng HY, Sun WJ, et al. Recognition of RNA N^6-methyladenosine by IGF2BP proteins enhances mRNA stability and translation [J]. Nat Cell Biol, 2018, 20: 285-295.

[5] Xie GY, Wu XN, Ling YY, et al. A novel inhibitor of N6-methyladenosine demethylase FTO induces mRNA methylation and shows anti-cancer activities [J]. Acta Pharm Sin B, 2022, 12: 853-866.

[6] Bi Z, Liu YH, Zhao YL, et al. A dynamic reversible RNA N^6-methyladenosine modification: current status and perspectives [J]. J Cell Physiol, 2019, 234: 7948-7956.

[7] Zaccara S, Ries RJ, Jaffrey SR. Reading, writing and erasing mRNA methylation [J]. Nat Rev Mol Cell Biol, 2019, 20: 608-624.

[8] Xu YR, Zhang W, Shen F, et al. YTH domain proteins: a family of m^{6}A readers in cancer progression [J]. Front Oncol, 2021, 11: 629560.

[9] Geuens T, Bouhy D, Timmerman V. The hnRNP family: insights into their role in health and disease [J]. Hum Genet, 2016, 135: 851-867.

[10] Hao PQ, Yu JJ, Ward R, et al. Eukaryotic translation initiation factors as promising targets in cancer therapy [J]. Cell Commun Signal, 2020, 18: 175.

[11] Fu Y, Dominissini D, Rechavi G, et al. Gene expression regulation mediated through reversible m^{6}A RNA methylation [J]. Nat Rev Genet, 2014, 15: 293-306.

[12] Shen DD, Wang B, Gao Y, et al. Detailed resume of RNA m^{6}A

demethylases [J]. Acta Pharm Sin B, 2022, 12: 2193-2205.

[13] Ramesh-Kumar D, Guil S. The IGF2BP family of RNA binding proteins links epitranscriptomics to cancer [J]. Semin Cancer Biol, 2022, 86: 18-31.

[14] Weng HY, Huang F, Yu ZJ, et al. The m^{6}A reader IGF2BP2 regulates glutamine metabolism and represents a therapeutic target in acute myeloid leukemia [J]. Cancer Cell, 2022, 40: 1566-1582.

[15] Fang H, Sun Q, Zhou J, et al. m^{6}A methylation reader IGF2BP2 activates endothelial cells to promote angiogenesis and metastasis of lung adenocarcinoma [J]. Mol Cancer, 2023, 22: 99.

[16] Hou PF, Meng S, Li ML, et al. LINC00460/DHX9/IGF2BP2 complex promotes colorectal cancer proliferation and metastasis by mediating HMGA1 mRNA stability depending on m^{6}A modification [J]. J Exp Clin Cancer Res, 2021, 40: 52.

[17] Tatekawa S, Tamari K, Chijimatsu R, et al. N^6-methyladenosine methylation-regulated polo-like kinase 1 cell cycle homeostasis as a potential target of radiotherapy in pancreatic adenocarcinoma [J]. Sci Rep, 2022, 12: 11074.

[18] Liu JD, Zhang NS, Zeng JJ, et al. N^6-methyladenosine-modified lncRNA ARHGAP5-AS1 stabilises CSDE1 and coordinates oncogenic RNA regulons in hepatocellular carcinoma [J]. Clin Transl Med, 2022, 12: e1107.

[19] Cai YQ, Wang YZ, Mao BJ, et al. Targeting insulin-like growth factor 2 mRNA-binding proteins (IGF2BPs) for the treatment of cancer [J]. Eur J Med Chem, 2024, 268: 116241.

[20] Moerke NJ, Aktas H, Chen H, et al. Small-molecule inhibition of the interaction between the translation initiation factors eIF4E and eIF4G [J]. Cell, 2007, 128: 257-267.

[21] Plöchl J. Ueber einige derivate der benzoylimidozimmtsäure [J]. Berichte, 1884, 17: 1616-1624.

[22] Jun EE. Ueber die condensation der hippursäure mit phtalsäure-anhydrid und mit benzaldehyd [J]. Justus Liebigs Ann Chem, 1893, 275: 1-8.

[23] Hantzsch A. Condensationsprodukte aus aldehydammoniak und ketonartigen verbindungen [J]. Berichte, 1881, 14: 1637-1638.